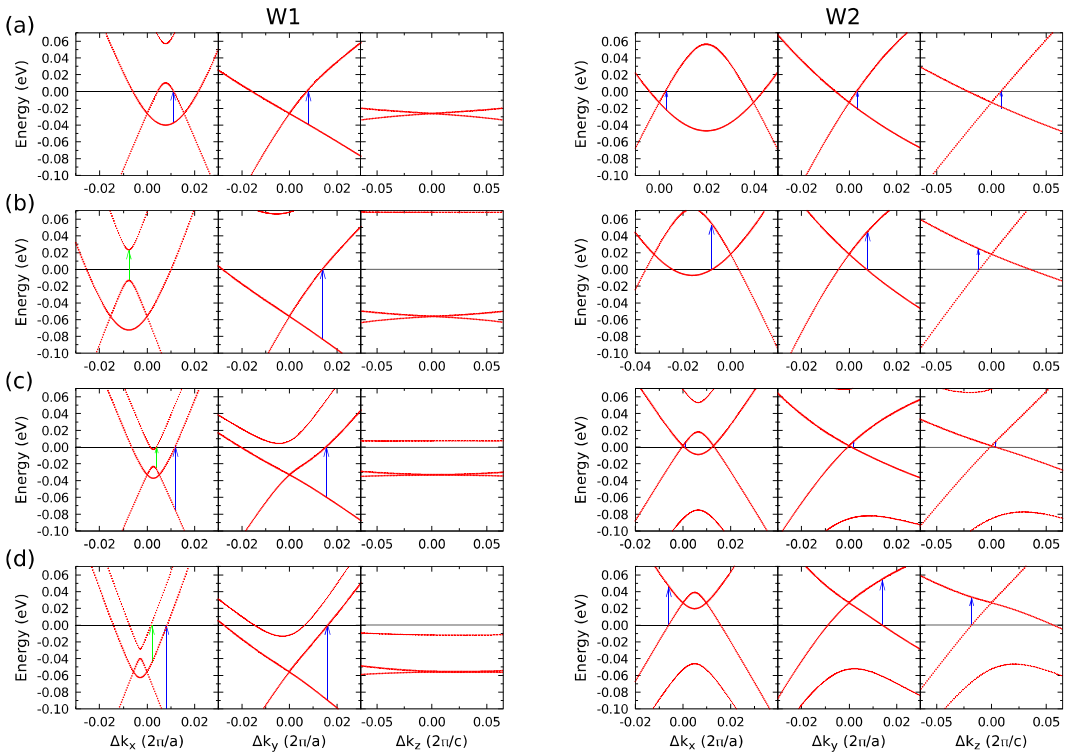

Figure 3. Bands (dotted red lines) around the Fermi level in a small energy interval close to the Weyl nodes in Table 2 in k_x, k_y, and k_z direction. The **k**-space location of the Weyl nodes is used as coordinate zero. The zero energy gives the Fermi level (horizontal black line). In the k_x case, pairs of Weyl nodes are displayed. The vertical arrows indicate possible onsets of the interband transitions in the vicinity of Weyl nodes. Blue arrows: transitions between Weyl bands; green arrows: transitions between Weyl and non-topological bands.

slightly larger value. ARPES measurements of TaAs show that the native chemical potential is very close to the energy of the W_2 Weyl nodes as in Fig. 3a and Table 2 [18]. For TaP it is estimated to be about 24 meV below the W_2 nodes[15]. For TaP, NbAs, and NbP our data in Table 2 reveal the coexistence of hole- and electron-type TWS pockets in the $k_z = 0$ plane (W_1) and in the $k_y = 0$ and $k_x = 0$ plane (W_2), respectively. This is experimentally confirmed for NbP by magnetoresistance measurements[20] and ARPES[16]. The measurement of the Fermi arcs by ARPES is more difficult for NbP[16]. The smaller SOI splitting decreases the separation of Weyl points compared to TaAs. The signs of ε_{F_i} in Table 2 show that the W_1 Weyl nodes give rise to eight electron pockets, while W_2 nodes are related to 16 hole pockets in the BZ. That means that the transition metal monopnictides possess a rather complex Fermi surface. TaAs represents an exception, because electron pockets also occur at W_2 nodes. Consequently, TaAs is not really a semimetal, rather a metal but with only a very low density of the conduction electrons.

The *ab initio* determination of the electron and hole densities from the computed bands is extremely difficult (see illustration in Fig. 3), because, in general, only a small surroundings of a Weyl node in **k** space contributes. Additionally, the closeness of the bands within one pair of Weyl nodes and the extremely flat W_1 bands parallel to the tetragonal axis (see Fig. 3) give rise to complications. The band linearity is restricted to small surroundings of $\mathbf{k}_W$ in reciprocal space. As a consequence, the Weyl fermion picture is limited to small energy intervals of the order of a few 10 meV. The accuracy of our computed values has been increased by using an extremely dense **k**-point meshes around the Weyl nodes characterized by a cutoff of $0.08 \times 2\pi/a$ or $2\pi/c$. The complex band structures between two Weyl nodes of a pair and the flat bands around W_1 points in tetragonal-axis direction as well as the resulting numerical uncertainties may be responsible for deviations from other calculations. Apart from TaAs the large hole densities for TaP, NbAs, and NbP computed in ref.[26] cannot be confirmed by our estimates using high **k** point densities around the Weyl nodes. The agreement is also difficult with densities extracted from experimental data. For NbP we estimate an electron density 0.1×10^{19} cm^{-3} by means of *the ab initio* method which is smaller than the value 2.5×10^{19} cm^{-3} derived within the effective-mass approximation (EMA) for both electrons and holes extracted from magnetotransport data[19]. Our band calculations (see Fig. 3 and its discussion), however, demonstrate that the EMA is hardly applicable. The extraction of carriers densities around Weyl nodes within the EMA from Hall measurements seems to tend to distinctly larger densities. Moreover, the carriers densities do not only depend on the method of their determination but also on the real structure of the samples. In addition, the presence of trivial hole pockets in the topological monopnictides may have strong influence on the measured carrier densities with an increasing tendency going from TaAs to NbP.

Weyl fermions. In Weyl semimetals of the transition metal monopnictide class the energies of the Weyl nodes in Table 2 differ only by a few meV, between 4 and 56 meV, from the Fermi level position. Consequently,